



# HHS Public Access

Author manuscript

*Ann N Y Acad Sci.* Author manuscript; available in PMC 2022 June 18.

Published in final edited form as:

*Ann N Y Acad Sci.* 2020 November ; 1480(1): 233–245. doi:10.1111/nyas.14514.

## A rabbit model for evaluating ocular damage from acrolein toxicity *in vivo*

Suneel Gupta<sup>1,2</sup>,

Michael K. Fink<sup>1,2</sup>,

Lynn M. Martin<sup>1,2</sup>,

Prashant R. Sinha<sup>1,2</sup>,

Jason T. Rodier<sup>1,3</sup>,

Nishant R. Sinha<sup>1,2</sup>,

Nathan P. Hesemann<sup>1,3</sup>,

Shyam S. Chaurasia<sup>1,2</sup>,

Rajiv R. Mohan<sup>1,2,3</sup>

<sup>1</sup>Harry S. Truman Memorial Veterans' Hospital, Columbia, Missouri

<sup>2</sup>One-Health Vision Research Program, Department of Veterinary Medicine & Surgery and Biomedical Sciences, College of Veterinary Medicine, University of Missouri, Columbia, Missouri

<sup>3</sup>Mason Eye Institute, School of Medicine, University of Missouri, Columbia, Missouri

### Abstract

Acrolein is a highly reactive and volatile unsaturated aldehyde commonly used for producing scores of commercial products. It has been recognized as a chemical weapon since its use during World War I, and more recently, in Syria. Acrolein exposure causes severe eye, skin, and lung damage in addition to many casualties. In the eye, it causes severe pain, eyelid swelling, corneal burns, and vision impairment. Very little information is available about how acrolein damages the cornea and causes vision loss. At present, the lack of clinically relevant animal models limits evaluation of acrolein toxicity and mechanisms specific to the eye. We aim to standardize the mode of delivery and exposure duration of acrolein, damaging the rabbit eye *in vivo* as an ocular injury model for studying the toxicity of acrolein and developing medical countermeasures. Rabbit eyes were exposed to two modes of delivery (topical and vapor) for different durations (1–5 minutes). Clinical ophthalmic examinations with a slit lamp, stereomicroscope, fluorescein dye, pachymeter, tonometer, and tearing examinations in live rabbits were performed at various times

---

Address for correspondence: Rajiv R. Mohan, Ph.D., FARVO, Professor of Ophthalmology and Molecular Medicine, One-Health Vision Research Program, Department of Veterinary Medicine & Surgery and Biomedical Sciences, College of Veterinary Medicine, University of Missouri, 1600 E. Rollins St, Columbia, MO 65211. MohanR@health.missouri.edu.

Author contributions

S.G. and M.K.F. performed animal studies, monitoring, slit-lamp eye examinations and imaging, clinical tests, cryopreservation, statistical analysis, and data collection, analysis, and management. P.R.S. and N.R.S. assisted with histology, immunofluorescence, and stereomicroscopy imaging. J.T.R., N.P.H., and L.M.M. performed clinical ophthalmic examinations in live animals. S.S.C. performed acrolein treatments, conceived the idea, provided feedback, and prepared the manuscript. R.R.M. conceived the idea, guided and supervised experiments, arranged for resources, and finalized the manuscript.

Competing interests

The authors declare no competing interests.

up to 4 weeks. Corneas were histologically diagnosed for transparency, fibrosis, collagens, and neovascularization. Our study successfully established an *in vivo* rabbit model for evaluating acrolein toxicity to the eye, accounting for different modes and durations of exposure.

## Keywords

cornea; acrolein; rabbit model; corneal dysfunction; ocular inflammation

## Introduction

Acrolein, a thiol-reactive electrophile, was used as a chemical weapon in World War I.<sup>1,2</sup> It is an important intermediate in the production of several commercial goods, including herbicides and pesticides. In the United States alone, over 500,000 tons of acrolein is produced and transported annually.<sup>3</sup> It is also released in the smoke from burning wood and forest fires and found in gasoline/diesel exhaust, and cigarette smoke.<sup>4</sup> In addition to the potential use of acrolein as a chemical weapon during World War I, its accidental spillage or hijacking by terrorists during transportation represents a very real domestic threat.

Acrolein is a strong irritant and causes severe pathologies in the eye, skin, and lungs.<sup>5-7</sup> In the eye, acrolein causes blindness due to ocular inflammation, pain, and corneal damage.<sup>2,3,5</sup> The cornea, an avascular and transparent outermost ocular tissue, protects the eye from injury and infection and provides 2/3 of refractive power to the eye.<sup>8,9</sup> Chemical exposure to the eye initiates a cascade of wound healing events and changes in the extracellular matrix (ECM) and collagen fibrils, whose unique arrangement is required for the maintenance of corneal transparency and function. Failure to heal properly will result in excessive inflammation, hyper cytokine and growth factor activity, disorganized collagen, stroma opacity, and an ingrowth of blood vessels (neovascularization) in the cornea.<sup>9</sup> We and other groups have identified significantly high levels of inflammatory cytokines, including interleukin (IL)-1 $\alpha$ , IL-1 $\beta$ , Fas ligand, and tumor necrosis factor- $\alpha$ , and growth factors such as transforming growth factor beta (TGF- $\beta$ ), epidermal growth factor (EGF), platelet-derived growth factor (PDGF), and vascular endothelial growth factor (VEGF), in rabbit corneas *in vivo* following surgical and chemical insult.<sup>9-13</sup> Drugs/agents inhibiting these factors arrest the development of corneal scarring and neovascularization significantly.<sup>13-15</sup> All these events lead to the increased myofibroblast accumulation and ECM deposition, causing corneal haze.<sup>9-15</sup> During the fibrotic repair stages, the cornea employs matrix metalloproteinases (MMPs) to degrade excessive ECM and remodel corneal collagens in order to restore transparency during wound healing.<sup>9-15</sup> There are currently only a few published studies that explain how acrolein causes corneal damage and vision loss because of the unavailability of clinically relevant animal models of acrolein's toxicity. How these deleterious effects are coordinated and result in corneal dysfunction are largely unknown so far.

In the present study, we sought to develop a preclinical *in vivo* rabbit model to better understand the ocular damage caused by acrolein in relation to the mode of delivery (topical versus vapor exposure) and duration of the exposure (1-5 min) for 28 days after the

exposure. The rabbit eye was chosen because of its similarity in size and anatomical features to the human eye in terms of dimensions, cellular composition, and physiological properties, except for the absence of the Bowman's layer. Furthermore, corneal wound healing events in rabbit eyes are similar to those in human eyes.<sup>16–18</sup> We found that topical or vapor application of acrolein severely damages the rabbit eye and causes a battery of ocular pathologies, including swelling of the eye, ocular surface abnormalities, inflammation, irregular collagen accumulation, and corneal opacity. In summary, we have established an *in vivo* rabbit model for studying acrolein toxicity to the eye. This model shows several clinical symptoms and parameters and the corneal damage, opacity, and wound healing events seen in human eyes.

## Materials and methods

### Chemicals and reagents

Acrolein (>99%, RCC150) was obtained from ULTRA Scientific Inc. (Thermo Fisher, Grand Island, NY) and used to evaluate acrolein-induced damage in ocular tissue. Topical artificial tears were purchased from the Rugby Laboratories, Livonia, MI. Sterile Weck-Cel ophthalmic spears were purchased from Beaver-Visitec International Inc., Waltham, MA. Surgical forceps, wire speculum, and sharp Westcott scissors were purchased from World Precision Instruments Inc., Sarasota, FL. Ketamine hydrochloride (JHP Pharmaceuticals, LLC, Rochester, MI), xylazine hydrochloride (XylaMed, Bimeda Inc., Oakbrook Terrace, IL), topical 0.5% proparacaine hydrochloride (Alcon, Ft. Worth, TX), and pentobarbital (Diamondback Drugs, Scottsdale, AZ) were obtained from the pharmacy of the Harry S. Truman VA Medical Center, Columbia, MO. Hematoxylin and eosin (H&E) solutions were procured from StatLab Medical Products, McKinney, TX. Balanced salt solution (BSS), 2-methylbutane, and antifade mounting medium containing 4',6-diamidino-2-phenylindole dihydrochloride (DAPI; cat # H1200, Vector Laboratories) were obtained from Thermo Fisher.

### Animals

The Institutional Animal Care and Use Committees of the University of Missouri and the Harry S. Truman Memorial Veterans' Hospital approved the study. Animals were treated in accordance with the ARVO Statement for the Use of Animals in Ophthalmic and Vision Research. Twenty-four New Zealand white rabbits (Charles River Laboratory Inc., Wilmington, MA) ranging from 4 to 5 pounds were procured and divided into four groups: vapor exposure for 1 min ( $n = 6$ ); vapor exposure for 3 min ( $n = 6$ ), topical exposure for 1 min ( $n = 6$ ); and topical exposure for 5 min ( $n = 6$ ). Both male and female rabbits were used and selected randomly for each group to avoid potential sex-based variability. Rabbits were housed in temperature-controlled ( $21 \pm 1$  °C) rooms with a light-dark cycle for 12 h and had ad libitum access to food and water. Rabbits were anesthetized with an intraperitoneal injection of a cocktail of ketamine hydrochloride (50 mg/kg) and xylazine hydrochloride (10 mg/kg) and received one or two drops of topical anesthetic, proparacaine hydrochloride (0.5%) onto the eye before acrolein exposure or clinical evaluation in order to minimize pain and discomfort to animals. Only one eye (left or right) of each animal was used for the

acrolein exposure assessment studies, and the unexposed eye served as control. Rabbits were thermally supported throughout the procedure and during the anesthetic recovery period.

### Acrolein exposure procedure

**Vapor delivery method.**—Acrolein vapors were dispensed to the rabbit eye for different times (1 or 3 min) to create moderate to severe injury. In brief, an 8-mm diameter filter paper disk containing acrolein (30  $\mu$ L) was placed in the center of the custom-made circular transparent polypropylene chamber and then positioned upside-down onto the rabbit eye for 1 or 3 min, as shown in Figure 1A. Vapors emitted from the filter paper disk in the enclosed chamber were in direct contact with the cornea/eye, mimicking a scenario encountered by humans in a real-life acrolein poisoning, except for the lack of eye blinking. Thereafter, the eye chamber was removed, and the eye was profusely washed with BSS (15–20 milliliters). The entire procedure was performed in a chemical hood in collaboration with ophthalmologists following all safety guidelines.

**Topical delivery method.**—Rabbit eyes were exposed to acrolein topically for two different times (1 or 5 min) using a filter paper disk to create mild/severe injury evenly in the targeted corneal area. In brief, an 8-mm diameter filter-paper disk soaked in acrolein (30  $\mu$ L) was applied onto the central cornea for 1 or 5 min as shown in Figure 1B. Thereafter, the filter paper disk was removed and the eye was thoroughly washed with BSS (15–20 milliliters). The entire procedure was performed in a chemical hood in collaboration with ophthalmologists following all safety guidelines.

### Clinical and biomicroscopy evaluations

The clinical evaluation and biomicroscopy imaging procedures were performed in live animals before and after acrolein injury at regular intervals (30 min and 1, 3, 7, 14, 21, and 28 days) under general anesthesia following consistent specifications to minimize variation. A slit-lamp microscope (Kowa, SL-15 portable slit lamp, Torrance, CA) fitted with a high-definition digital imaging system (Kowa, portable VK-2 Ver. 5.50) was used to record clinical ocular health assessment data. A stereomicroscope (Leica MZ16F, Leica Microsystems Inc., Buffalo Grove, IL) equipped with a digital camera (SpotCam RT KE, Diagnostic Instruments Inc., Sterling Heights, MI) was used to access and record the levels of ocular damage from acrolein following our reported protocol. All *in vivo* clinical examinations were performed at least by two or more independent investigators (S.G., M.K.F., L.M.M., J.T.R., and N.P.H.) in a blinded manner following the Roper-Hall classification providing prognostic guidelines based on the level of corneal involvement and limbal ischemia.<sup>19</sup> Eyes were kept moist with artificial tears during the entire procedure to prevent corneal desiccation.

Corneal epithelial defects were observed with a commercial ophthalmic fluorescein stain (Altafluor Benox). The epithelial defects were assessed under a cobalt light blue filter and recorded under a GFP light filter using a slit-lamp microscope equipped with an image capturing system (Leica MZ16F, Leica Microsystems Inc.) using with a digital camera (SpotCam RT KE, Diagnostic Instruments Inc.). The clinical findings were documented by photography and scored by a minimum of two independent researchers and clinicians (S.G.,

M.K.F., L.M.M., J.T.R., and N.P.H.) in a blinded fashion. The size of corneal epithelial defects in rabbit eyes was digitally computed by counting pixels of the defect areas in images taken with stereomicroscope at 7.1× magnification using ImageJ and Photoshop software following the procedure reported earlier.<sup>20–22</sup>

An ultrasonic pachymeter (Accutome, AccuPach VI Pachymeter) was used to assess corneal edema and thickness under general anesthesia before and after acrolein exposure at 30 min and 1, 7, 14, 21, and 28 days. A handheld tonometer (Tono-Pen AVIA® Tonometer) was used to record changes in intraocular pressure (IOP) at all tested times. Schirmer tear test strips (Fisher Scientific) were used to quantify tear volume at each time point in live animals.

### Ocular tissue collection

Rabbits were humanely euthanized at the termination point with an intraperitoneal injection of pentobarbital (150 mg/kg) while animals were under general anesthesia. Eyes were enucleated with surgical forceps and Westcott scissors under a dissecting microscope (Leica Wild M690, Leica Microsystems Inc.). The corneal tissues were immediately placed into molds containing optimal cutting temperature compound and snap frozen in a container of 2-methylbutane immersed in liquid nitrogen. Frozen tissues were maintained at –80 °C until sectioning and further evaluation. Tissues were sectioned at 8-µm thickness with a cryomicrotome, mounted on glass microscope slides, and stored at –80 °C for subsequent analysis.

### Histopathological evaluations

Acrolein-exposed and -nonexposed rabbit corneal tissue sections were subjected to H&E staining to record and assess morphological alterations after acrolein exposure. H&E staining was performed in our laboratory using the protocol reported previously.<sup>22,23</sup> Additionally, corneal sections were also sent to the Veterinary Medical Diagnostic Laboratory at the University of Missouri (MU) for H&E histology.

### Masson's trichrome staining

Control and acrolein-exposed rabbit corneal tissue sections were subjected to Masson's trichrome staining to evaluate alterations in collagen, a primary component of the ECM. Masson's trichrome staining was performed independently within the laboratory and by the MU Veterinary Medical Diagnostic Laboratory using reported protocol.<sup>22,23</sup>

### Immunofluorescence staining

DAPI staining was additionally used to visualize cellular density by analyzing DAPI-stained nuclei in corneal tissue sections prepared from control and acrolein-exposed eyes under a fluorescence microscope. In brief, frozen corneal tissue sections were left at room temperature for 15 min and then washed three times (5 min each) with 1× PBS. Excess fluid from tissue sections was removed using Kimwipes, a drop of DAPI antifade Vectashield medium (H1200) was applied, and sections were mounted with premier coverslips (Thermo Fisher). The stained sections were viewed and photographed with a fluorescence microscope

(Leica DM 4000B, Leica Microsystems Inc.) equipped with a digital camera (SpotCam RT KE, Diagnostic Instruments Inc.).

### Statistical analysis

Statistical analysis was performed using GraphPad Prism 6.07 software (GraphPad, La Jolla, CA). Student's *t*-test and two-way analysis of variance (ANOVA) with the Wilcoxon rank sum test or the Bonferroni multiple comparison post-hoc test were used depending on research design for all clinical data collected for IOP, corneal thickness, and ocular fluid. Values of  $P < 0.05$  were considered statistically significant.

## Results

### Stereobiomicroscopy

Acrolein exposure to the rabbit eye caused severe damage to the eyelids, cornea, and conjunctiva in a time-dependent manner, depending on the mode of delivery. Vapor exposure for 1 min (Fig. 2B–F) and 3 min (Fig. 2H–L) caused severe eyelid swelling and inflammation at 30 min and continued up to 28 days compared with the untreated control groups (Fig. 2A and G). All acrolein-treated eyes in the vapor-exposed group showed notably high ocular morbidity, as indicated by increased eyelid inflammation and corneal opacity throughout the experimental protocol (28 days). The peak eyelid swelling was observed 1 day after acrolein injury in both the 1- and 3-min vapor-exposed eyes. Similarly, topical exposure resulted in severe eyelid swelling (but relatively less than the vapor exposure group), intense ocular inflammation, and dense corneal opacity in the early stages of the injury (30 min to 14 days) in the 1-min (Fig. 2N–P) and 5-min (Fig. 2T and U) exposure groups but subsequently decreased gradually over time by 21 days (Fig. 2Q and W) and 28 days (Fig. 2R and X). The morbidity in these animals was significantly high compared with the untreated control groups. Additionally, we observed sprouting of neovessels into the rabbit cornea from the conjunctiva at day 14 after topical acrolein exposure for the 1-min (Fig. 2P–R) and 5-min (Fig. 2V–X) topically exposed groups. Interestingly, neither the 1-min (Fig. 2B–F) nor 3-min (Fig. 2H–P) acrolein vapor-exposed group showed ingrowth of neovessels into the rabbit cornea from the conjunctiva (neovascularization).

Regardless of the mode of exposure (vapor or topical), acrolein contact to the eye caused significantly excessive tear secretion and corneal edema in all acrolein-exposed eyes compared with non-treated control eyes. Interestingly, IOP remained unchanged following topical exposure, whereas IOP increased significantly up to day 7 in the 1-min and up to day 14 in the 3-min vapor exposure groups. Table 1 shows the levels of the inspected clinical parameters for the various treatments at the tested time points and their statistical analysis ( $P$  values).

### Slit-lamp microscopy

Slit-lamp microscopy was used to clinically evaluate ocular health, inflammation, corneal opacity, and neovascularization (Fig. 3). Acrolein vapor exposure for 1 min (Fig. 3B) and 3 min (Fig. 3H) resulted in increased corneal opacity after 30 min, which increased

significantly with time and showed grade IV clinical haze throughout the study (Fig. 3C–F). On the other hand, the topical application of acrolein caused morbid levels of ocular inflammation within 30 min of topical exposure (Fig. 3N and T) that gradually declined with time. Severe haze appeared at day 7 (Fig. 3O and U) and resulted in clinical grade III damage to eyes observed up to day 28 (Fig. 3P–R and V–X) compared with the control groups (Fig. 3M and S). In the later phase of wound healing (days 14–28), the topically applied acrolein group progressively developed corneal opacity, prominent scarring, and neovascularization, independent of duration (Fig. 3). The semiquantification of subjective *in vivo* clinical eye examinations done employing the prognostic guidelines of the Roper-Hall classification for the vapor exposure (1- or 3-min) group ranged from grade I to II during the early stages after corneal injury (30 min to day 7) but advanced to grade III or IV at later times (from day 7 to day 28). Contrary to the increasing damage observed in the vapor-exposed group, the damage to the rabbit eye did not exceed grade II in the topically exposed group at any tested time point (ranging from grade I to II from 30-min to day 21 and mostly grade I on day 28).

### Fluorescein dye staining

Acrolein exposure compromises ocular surface healing in both the vapor and topical mode of delivery (Fig. 4). Fluorescein dye staining revealed that the acrolein vapor-exposed groups experienced the maximum erosion and abrasion on the ocular surface tissue in 1-min (Fig. 4B–F) and 3-min (Fig. 4H–L) exposed eyes as the corneal epithelium in these rabbits failed to heal completely after 28 days compared with the control groups (Fig. 4A and G). In the topical acrolein-exposed rabbit eyes, corneal epithelial cells showed delayed healing response in the 1-min (Fig. 4N–R) and 5-min treated groups (Fig. 4T–X). Under physiological conditions, damaged corneal epithelium typically heals fully within 3 days. The extent of corneal epithelial injury in rabbit eyes in the vapor-exposed group ranged from 58% to 96% ± 16% for various tested time points (30 min to day 28). In general, damage to corneas/eyes exposed to vapor for 3 min (Fig. 4H–L) was more than the eyes exposed for 1 min (Fig. 4B–F). Contrary to these real-time clinical findings, the corneal epithelial damage in rabbit eyes after topical acrolein exposure was notably less (14–39% ± 9%) and lasted until day 7 (Fig. 4N and O), with nearly 100% epithelial recovery by day 14 in the 1-min topical exposure group (Fig. 4P–R) and 90–95% in the 5-min topical exposure group (Fig. 4V–X).

### Fluorescence staining of nuclei

To test whether acrolein toxicity caused cellular damage to the corneal keratocytes and migration of infiltrating inflammatory cells, we collected rabbit corneas 28 days after acrolein vapor or topical exposure and stained them with DAPI to visualize the nuclei of all cells within the tissue. The cornea consists of six layers of epithelial cells, keratocytes in the stroma, and a single-layer endothelium. Figure 5 shows a substantial decrease in DAPI-stained nuclei in the epithelium and anterior stroma in the corneas of the vapor-exposed group (1 and 3 minutes). Conversely, there was markedly less damage to the corneal epithelium and stroma in the eyes of topically exposed group than the vapor-exposed group. The eyes topically exposed to acrolein for 5 min showed notably less damage to the epithelium and anterior stroma compared with the eyes topically exposed for 1 minute.

Additionally, we observed severely compromised corneal endothelium in acrolein-exposed eyes compared with the nonexposed control eyes. The damage to the endothelium was more pronounced in the vapor-exposed eyes compared with the topically exposed eyes. It is likely that some of the DAPI-stained cells may be inflammatory cells infiltrating into the anterior stroma closer to the wound site. These data suggest that acrolein causes significant damage to all three major cell types in the rabbit cornea *in vivo*.

### Histological evaluation

The corneal tissues collected from both vapor and topical exposure groups were sectioned and stained with H&E in order to visualize inflammatory cells, acellular space, and neovascularization (Fig. 6) 28 days after acrolein exposure. We observed a significant accumulation of migrating inflammatory cells beneath the site of injury in the anterior stroma in the 1-min acrolein vapor-exposed eyes. The epithelium of the acrolein vapor-exposed eyes showed considerable thinning in the corneal epithelium as compared with the control eyes. The increase in exposure time from 1 to 3 min disrupted cellular corneal architecture and created numerous acellular spaces in the corneal stroma. This histopathological data revealed that acrolein's toxicity to the cornea is dose dependent. Topical exposure of acrolein for 1 min to the eye caused notably increased infiltration of the inflammatory cells into the anterior stroma and loss of cells in the posterior stroma. These pathological conditions became more severe in the 5-min topical exposure eyes as evident from the acellular zone in the anterior stroma, loss of keratocytes, infiltration of a large number of inflammatory migratory cells, and distortion of the cellular architecture (Fig. 6).

### Masson's trichrome staining

Acrolein treatment of the eye via vapor or topical application severely compromised corneal transparency, ECM organization, and collagen levels and organization (Fig. 7). In both the acrolein vapor- and topical-exposed eyes, the Masson's trichrome staining revealed that the corneal stromal layers experienced edema, morphological alterations, and a dramatic change in collagen amount and arrangement after acrolein exposure. The changes in collagen levels are depicted by the blue color intensity and were found to be more predominant in the longer acrolein exposure times for both the vapor- and topically exposed eyes. In general, acrolein vapor-exposed eyes demonstrated much increased irregularities in collagen deposition in the corneal stroma than the topically exposed eyes. The biggest increase in stromal collagen was seen in the 3-min vapor-exposed corneas. The collagen and ECM alterations in both the vapor and topical exposure groups were further confirmed by the Masson's trichrome staining.

### Discussion

Acrolein is a highly reactive unsaturated aldehyde and a strong vesicant that causes severe health disorders in the eye, lung, and other tissues.<sup>4-7</sup> It had been used as a chemical since World War I and can be used as a weapon by terrorists.<sup>1-3</sup> At this time, limited literature describing the mechanism and lack of clinically relevant *in vivo* models are the major barriers for the development of medical countermeasures to treat ocular damage and vision impairment caused by acrolein poisoning. Acrolein contact to the eye in humans causes



severe ocular pain, lacrimation, blepharconjunctivitis, eyelid swelling, corneal burns and opacity, and vision loss.<sup>2,3,5</sup> Very little information is available about how acrolein damages eyelid tissues and the cornea, which results in vision loss. Dachir *et al.* determined the thresholds for acute irritation by acrolein toxicity in rabbits and found that exposure of the eye to acrolein vapor may result in excess tearing, corneal erosions, and neovascularization.<sup>5</sup> Furthermore, these authors found a reduction in the severity of acrolein poisoning in rabbit eyes after anti-inflammatory treatment combined with a short-term topical local anesthetic.<sup>5</sup> A similar study in human volunteers found minor subjective eye irritation after a short exposure to acrolein under controlled conditions.<sup>24</sup> Another human study of exposure to acrolein suggested a time- and individual-dependent variation in the eye irritation.<sup>25</sup> All these studies were limited in scope and emphasized the need for a clinically relevant *in vivo* ocular model of acrolein toxicity. In the present study, we successfully established an *in vivo* rabbit ocular model of acrolein toxicity. We selected the seven most relevant time points (30 min and 1, 3, 7, 14, 21, and 28 days) based on our previously published data on corneal wound healing.<sup>17,18,22,23,26</sup> We optimized two different modes of exposure (vapor and topical) that represent real-world situations. Next, we standardized two different times of exposure (1 and 3 min for vapor exposure and 1 and 5 min for topical exposure) and its effect on ocular damage and vision loss. Acrolein caused severe eyelid swelling, excessive tearing, and increased inflammation within 30 min of exposure and noteworthy corneal edema, corneal opacity, and neovascularization subsequently. These pathological features were dependent on the mode of delivery as well as the timing of exposure throughout the experiment (up to day 28). The most striking information from our data is that according to most of the examined parameters, the same amount of acrolein exposure to the eye in the form of vapor caused more damage compared with the topical treatment, which was contrary to our initial expectation. Furthermore, we did not note any differences in the clinical or histological parameters between male and female rabbits. This observation is consistent with our previous report that showed that sex is not a biological variable in corneal wound healing in the rabbit model.<sup>17</sup>

A single exposure to acrolein by vapor or topically caused a massive wave of anterior segment trauma within 30 minutes. The clinical parameters observed include inflamed and swollen eyelids (also known as blepharitis), a significant spike in the IOP in the eyes of the 1-min vapor exposure group lasting until day 7 and until day 14 in the 3-min vapor exposure group, excessive tear volume, and corneal edema. Also, we observed physical damage to the eyes and periocular structures, including lacerations, abrasions, conjunctival swelling, and ocular surface defects, a relatively more severe scenario in the vapor-exposed eyes compared with topical exposure. Histological evaluation of day 28 corneal tissue sections showed disrupted morphology in all three corneal layers—the epithelium, stroma, and endothelium—by H&E staining. Acrolein exposure by vapor caused severe ocular surface abrasions in the epithelial cell layers, as seen with fluorescein staining. The corneal epithelium was severely damaged in the 1-min exposed group, which further deteriorated in the 3-min exposed group and completely failed to heal at the end of experimental study (day 28). We also observed thinning of epithelial cells and signs of possible limbal cell deficiency in the vapor-exposed corneal tissues. On the other hand, topical exposure of acrolein showed delayed epithelial healing, with few spots of epithelial defects in the

fluorescein-stained corneas even at day 28, which was also seen in the H&E-stained corneal sections. Nonetheless, there remains a speculative possibility that topically applied local anesthesia on the eye might have influenced the toxicological effect of the acrolein.

Clinical and histological analysis showed significant changes in corneal tissue morphology at day 28 after acrolein exposure for both the vapor and topical exposure methods. Wound healing after injury plays an essential role in corneal and other ocular tissue repair. Keratocytes are a major cell type in the corneal stroma that regulates corneal clarity, homeostasis, and function.<sup>27–31</sup> Keratocytes are typically quiescent but acquire repair phenotypes after injury/infection and perform wound repair.<sup>27</sup> The extent of healing depends on the level of keratocyte migration, proliferation, and differentiation to fibroblasts and myofibroblasts.<sup>28–33</sup> The corneal wound healing process is primarily controlled by epithelial–stromal interactions, cytokines and their receptors, and inflammatory factors.<sup>9,18,30–32</sup> Many researchers have reported the expression and involvement of various growth factors, including TGF- $\beta$ , VEGF, EGF, and their receptors in corneal scarring, neovascularization, and wound healing *in vivo*.<sup>9–15</sup> Additionally, the role of proinflammatory cytokines, chemokines, MMPs, and ECM-remodeling enzymes has also been well documented in corneal wound healing.<sup>13–15</sup> Immediately after chemical injury, the cornea and eyelids exhibit infiltration of inflammatory cells, such as neutrophils and macrophages, which secrete large quantities of lipid mediators, including leukotrienes.<sup>33–36</sup> Furthermore, epithelial cells of the meibomian glands in the eyelid secrete large quantities of leukotrienes and mucus in response to chemical injury.<sup>35,36</sup> Leukotrienes enhance vascular permeability, promote neutrophil recruitment, and increase cytokine levels, which cause ocular edema, inflammation, and possibly limbal stem cell deficiency.<sup>36</sup> The clinical and gross histopathological examinations of this study prompted us to postulate involvement of these factors in acrolein's toxicity to the eye. Our ongoing cellular and molecular studies are investigating such possibilities and potential mechanisms that could be targeted for arresting toxicity and/or developing medical countermeasures.

We found significant alterations in the stromal layer, including edema, presence of leucocytes, and infiltration by inflammatory cells. Stereomicroscopy images showed severe morbidity in ocular tissues characterized by corneal opacity and neovascularization (ingrowth of new vessels) at day 14 after ocular acrolein exposure and which continued until day 28 at the time of tissue collection (Figs. 2–7). Interestingly, neovascularization was more prominent in the topically exposed corneas compared with the vapor-exposed eyes in which corneal haze/opacity was more pronounced. Histological evaluation using H&E provided similar observations, where more corneal fibrosis was seen in the vapor-exposed group compared with the topically exposed group. We predict that this was likely due to a significant inflow of migrating inflammatory cells in the topically treated corneas, which results in neovascularization and partial clearance of corneal haze in the late stages of wound healing (day 14 up to day 28). Conversely, we found increased corneal opacity (by stereomicroscopy) and haze (by slit-lamp microscopy) with time in the vapor-exposed eyes, which persistently increased throughout the study with a lesser amount of inflammation and neovascularization (day 28). This differing pathological phenomenon can be instrumental in designing and developing newer, safe, and effective interventional strategies to treat patients exposed to vapor and/or topical acrolein.

The corneal stroma has a unique structural property governed by its main dry constituent, collagen, which provides a high level of transparency to visible wavelengths.<sup>37,38</sup> Any injury to the cornea disrupts the integrity of collagen fibril organization and spatial arrangement in the stroma.<sup>39–41</sup> One of the most important characteristics of the corneal wound healing mechanism is the reorganization of ECM, including corneal collagens, which increases corneal structural integrity and transparency.<sup>42–44</sup> We used Masson's trichrome dye to stain the collagens in the corneal sections collected on day 28. Acrolein-treated corneas showed significantly high levels of collagen deposition, which is seen by the increased intensity of the blue color in the corneal stroma. This is supported by the observed disintegrated corneal tissue cell architecture in the histological evaluation and Mason's trichrome staining. Of note, we found a higher density of collagens in the acrolein vapor-exposed corneal stroma compared with the topically exposed group. This unique observation demands further investigation of ultrastructural features by transmission electron microscopy.

In summary, it is imperative to have effective antidotes for accidental acrolein exposure during an industrial spill or intentional misuse of acrolein by terrorists. The development of proper tools for effective countermeasures against chemicals is a priority research area identified by the U.S. government after the 9/11 terrorist attacks. Accordingly, we have established a clinically relevant *in vivo* rabbit model based on different modes and durations of ocular exposure that recapitulates many clinical symptoms of acrolein's toxicity, such as blepharitis, ocular surface damage, corneal opacity, inflammation, and neovascularization, typically seen in human eyes. The optimized rabbit model is simple, easy to use in a laboratory setting, and suitable for carrying out mechanism-based toxicity studies and evaluating the therapeutic potential of novel agents and existing drugs to mitigate acrolein's toxicity to the eye.

## Acknowledgments

This work was primarily supported by the NEI, NIH 5R21EY030233 Grant (R.R.M.) and partially by a pilot grant (S.G.) from the Truman VA Medical Research Foundation, Columbia, Missouri, USA; 5R21EY030234, 5R01EY017294, and 1R01EY030774 Grants (R.R.M.) from the National Eye Institute, NIH, Bethesda, Maryland, and 1101BX000357 Merit and RCS Grants (R.R.M.) from the United States Veterans Health Affairs, Washington, DC. S.S.C. is supported by the NEI, NIH R01EY029795 Grant.

## References

1. Beauchamp RO Jr., Andjelkovich DA, Kligerman AD, et al. 1985. A critical review of the literature on acrolein toxicity. *Crit. Rev. Toxicol.* 14: 309–380. [PubMed: 3902372]
2. Grant WM 1974. *Toxicology of the Eye: Drugs, Chemicals, Plants, Venoms*. Springfield, IL: Thomas.
3. Ronald E 2007. *Eisler's Encyclopedia of Environmentally Hazardous Priority Chemicals*. 1st ed. Amsterdam: Elsevier.
4. Kehrer JP & Biswal SS. 2000. The molecular effects of acrolein. *Toxicol. Sci.* 57: 6–15. [PubMed: 10966506]
5. Dachir S, Cohen M, Gutman H, et al. 2015. Acute and long-term ocular effects of acrolein vapor on the eyes and potential therapies. *Cutan. Ocul. Toxicol.* 34: 286–293. [PubMed: 25363068]
6. Takeuchi K, Kato M, Suzuki H, et al. 2001. Acrolein induces activation of the epidermal growth factor receptor of human keratinocytes for cell death. *J. Cell Biochem.* 81: 679–688. [PubMed: 11329622]

7. Feng Z, Hu W, Hu Y, et al. 2006. Acrolein is a major cigarette-related lung cancer agent: preferential binding at p53 mutational hotspots and inhibition of DNA repair. *Proc. Natl. Acad. Sci. USA* 103: 15404–15409. [PubMed: 17030796]
8. Ma DH, Chen HC, Lai JY, et al. 2009. Matrix revolution: molecular mechanism for inflammatory corneal neovascularization and restoration of corneal avascularity by epithelial stem cell transplantation. *Ocul. Surf.* 7: 128–144. [PubMed: 19635246]
9. Wilson SE, Mohan RR, Mohan RR, et al. 2001. The corneal wound healing response: cytokine-mediated interaction of the epithelium, stroma, and inflammatory cells. *Prog. Retin. Eye Res.* 20: 625–637. [PubMed: 11470453]
10. Mohan RR, Tandon A, Sharma A, et al. 2011. Significant inhibition of corneal scarring *in vivo* with tissue-selective, targeted AAV5 decorin gene therapy. *Invest. Ophthalmol. Vis. Sci.* 52:4833–4841. [PubMed: 21551414]
11. Tandon A, Tovey TC, Sharma A, et al. 2010. Role of transforming growth factor beta in corneal function, biology and pathology. *Curr. Mol. Med.* 10: 565–578. [PubMed: 20642439]
12. Saika S, Yamanaka O, Sumioka T, et al. 2010. Transforming growth factor beta signal transduction: a potential target for maintenance/restoration of transparency of the cornea. *Eye Contact Lens* 36: 286–289. [PubMed: 20823707]
13. Maddula S, Davis DK, Maddula S, et al. 2011. Horizons in therapy for corneal angiogenesis. *Ophthalmology* 118: 591–599. [PubMed: 21376242]
14. Tandon A, Tovey JC, Waggoner MR, et al. 2012. Vorinospotent agent to prevent and treat laser-induced corneal haze. *J. Refract. Surg.* 28: 285–290. [PubMed: 22386369]
15. Sharma A, Bettis DI, Cowden JW, et al. 2010. Localization of angiotensin converting enzyme in rabbit cornea and its role in controlling corneal angiogenesis *in vivo*. *Mol. Vis.* 16: 720–728. [PubMed: 20431722]
16. Zernii EY, Baksheeva VE, Iomdina EN, et al. 2016. Rabbit models of ocular diseases: new relevance for classical approaches. *CNS Neurol. Disord. Drug Targets* 15: 267–291. [PubMed: 26553163]
17. Tripathi R, Giuliano EA, Gafen HB, et al. 2019. Is sex a biological variable in corneal wound healing? *Exp. Eye Res.* 187:107705. [PubMed: 31226339]
18. Mohan RR, Hutcheon AEK, Choi R, et al. 2003. Apoptosis, necrosis, proliferation, and myofibroblast generation in the stroma following LASIK and PRK. *Exp. Eye Res.* 76: 71–87. [PubMed: 12589777]
19. Roper-Hall MJ 1965. Thermal and chemical burns. *Trans. Ophthalmol. Soc. U.K.* 85: 631–653. [PubMed: 5227208]
20. Mohan RR, Schultz GS, Hong JW, et al. 2003. Gene transfer into rabbit keratocytes using AAV and lipid mediated plasmid DNA vectors with a lamellar flap for stromal access. *Exp. Eye Res.* 76: 373–383. [PubMed: 12573666]
21. Mohan RR, Tripathi R, Sharma A, et al. 2019. Decorin antagonizes corneal fibroblast migration via caveola-mediated endocytosis of epidermal growth factor receptor. *Exp. Eye Res.* 180: 200–207. [PubMed: 30611736]
22. Gupta S, Fink MK, Ghosh A, et al. 2018. Novel combination BMP7 and HGF gene therapy instigates selective myofibroblast apoptosis and reduces corneal haze *in vivo*. *Invest. Ophthalmol. Vis. Sci.* 59:1045–1057. [PubMed: 29490341]
23. Gronkiewicz KM, Giuliano EA, Kuroki K, et al. 2015. Development of a novel *in vivo* corneal fibrosis model in the dog. *Exp. Eye Res.* 143: 75–88. [PubMed: 26450656]
24. Dwivedi AM, Johanson G, Lorentzen JC, et al. 2015. Acute effects of acrolein in human volunteers during controlled exposure. *Inhal. Toxicol.* 27: 810–821. [PubMed: 26635308]
25. Claeson AS & Lind N. 2016. Human exposure to acrolein: time-dependence and individual variation in eye irritation. *Environ. Toxicol. Pharmacol.* 45: 20–27. [PubMed: 27235799]
26. Tandon A, Sharma A, Rodier JT, et al. 2013. BMP7 gene transfer via gold nanoparticles into stroma inhibits corneal fibrosis *in vivo*. *PLoS One* 8: e66434. [PubMed: 23799103]
27. West-Mays JA & Dwivedi DJ. 2006. The keratocyte: corneal stromal cell with variable repair phenotypes. *Int. Biochem. Cell Biol.* 38: 1625–1631.

28. Hassell JR & Birk DE. 2010. The molecular basis of corneal transparency. *Exp. Eye Res.* 91: 326–335. [PubMed: 20599432]
29. Fini ME & Stramer BM. 2005. How the cornea heals: cornea-specific repair mechanisms affecting surgical outcomes. *Cornea* 4: S2–S11.
30. Wilson SE 2012. Corneal myofibroblast biology and pathobiology: generation, persistence, and transparency. *Exp. Eye Res.* 99: 78–88. [PubMed: 22542905]
31. Wilson SE, Liu JJ & Mohan RR. 1999. Stromal-epithelial interactions in the cornea. *Prog. Retin. Eye Res.* 18:293–309. [PubMed: 10192515]
32. Gupta S, Rodier JT, Sharma A, et al. 2017. Targeted AAV5-Smad7 gene therapy inhibits corneal scarring *in vivo*. *PLoS One* 12: e0172928. [PubMed: 28339457]
33. Bazan HE 2005. Cellular and molecular events in corneal wound healing: significance of lipid signaling. *Exp. Eye Res.* 80:453–463. [PubMed: 15781273]
34. Hurst JS, Balazy M, Bazan HE, et al. 1991. The epithelium, endothelium, and stroma of the rabbit cornea generate (12S)-hydroxyeicosatetraenoic acid as the main lipoxy-genase metabolite in response to injury. *J. Biol. Chem.* 266: 6726–6730. [PubMed: 1901855]
35. Gronert K 2005. Lipoxins in the eye and their role in wound healing. *Prostaglandins Leukot. Essent. Fatty Acids* 73: 221–229. [PubMed: 15979295]
36. Sahin A, Kam WR, Darabad RR, et al. 2012. Regulation of leukotriene B4 secretion by human corneal, conjunctival, and meibomian gland epithelial cells. *Arch. Ophthalmol.* 130: 1013–1018. [PubMed: 22893071]
37. Meek KM & Knupp C. 2015. Corneal structure and transparency. *Prog. Retin. Eye Res.* 49: 1–16. [PubMed: 26145225]
38. Quantock AJ & Young RD. 2008. Development of the corneal stroma, and the collagen–proteoglycan associations that help define its structure and function. *Dev. Dyn.* 237: 2607–2621. [PubMed: 18521942]
39. Holmes DF, Lu Y, Starborg T, et al. 2018. Collagen fibril assembly and function. *Curr.Top.Dev.Biol.*130: 107–142. [PubMed: 29853175]
40. Meek KM & Boote C. 2004. The organization of collagen in the corneal stroma. *Exp. Eye Res.* 78: 503–512. [PubMed: 15106929]
41. Meek KM & Fullwood NJ. 2001. Corneal and scleral collagens—a microscopist’s perspective. *Micron* 32: 261–272. [PubMed: 11006506]
42. Ljubimov AV & Saghizadeh M. 2015. Progress in corneal wound healing. *Prog. Retin. Eye Res.* 49: 17–45. [PubMed: 26197361]
43. Chen S, Mienaltowski MJ & Birk DE. 2015. Regulation of corneal stroma extracellular matrix assembly. *Exp. Eye Res.* 133: 69–80. [PubMed: 25819456]
44. Torricelli AA & Wilson SE. 2014. Cellular and extracellular matrix modulation of corneal stromal opacity. *Exp. Eye Res.* 129: 151–160. [PubMed: 25281830]

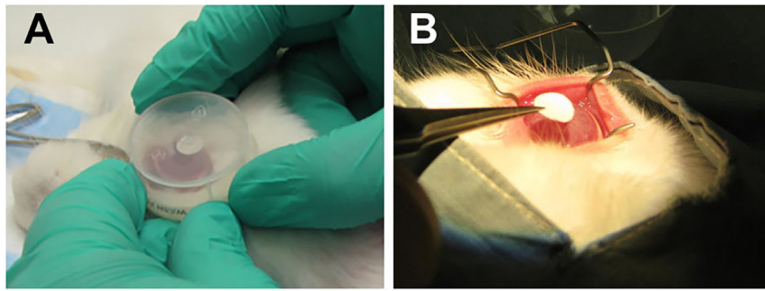


**Figure 1.** Experimental setup for the acrolein treatment via (A) vapor exposure and (B) topical exposure onto the rabbit eye.  $n = 6$  rabbit eyes in each group.

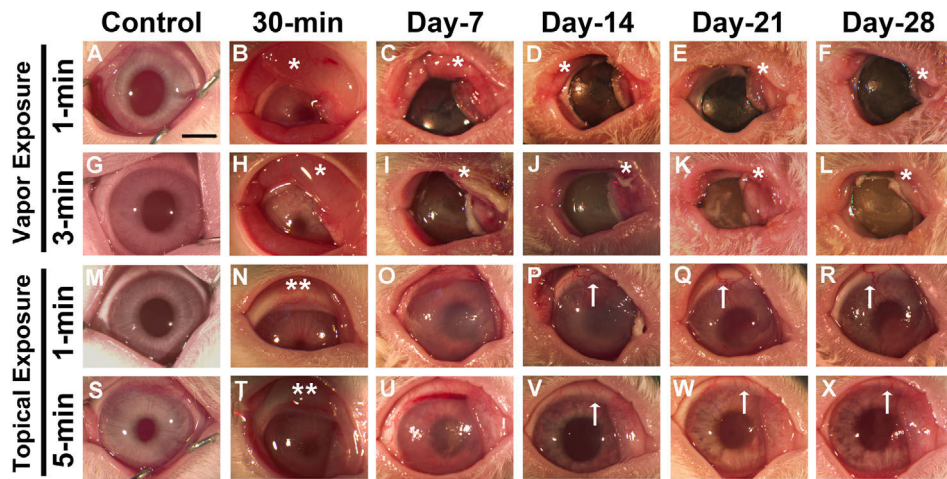


**Figure 2.**

*In vivo* stereobiomicroscopy images showing severe ocular damage in rabbit eyes from 30 min to 28 days following acrolein vapor exposure for 1 min (B–F) and 3 min (H–L) and topical exposure for 1 min (N–R) and 5 min (T–X). Panels A, G, M, and S are images of control nonexposed rabbit eyes. Vapor exposure to the cornea caused severe eyelid inflammation (\*) and corneal opacity. Abscesses appeared in the conjunctival region, and there was severe corneal haze and an opaque corneal surface. Topical exposure to the eyes caused mild eyelid inflammation (\*\*) in the early phase and prominent neovascularization (↑) in the late stages (14–28 days) of corneal wound healing.  $n = 6$  rabbit eyes in each group. All images were taken at  $7.1\times$  magnification. Scale bar = 3.0 mm.

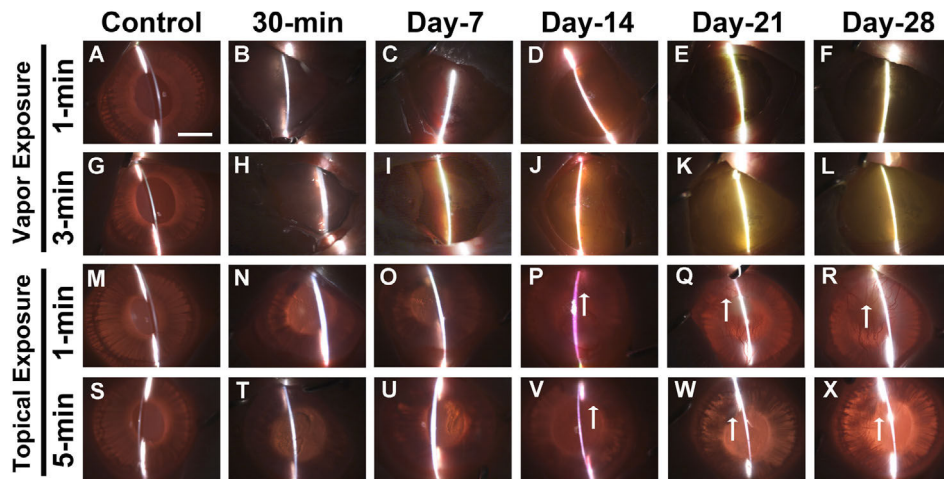


**Figure 3.**

*In vivo* slit-lamp biomicroscopy images showed severe ocular opacity in the rabbit eyes from 30 min to 28 days after acrolein vapor exposure for 1 min (B–F) and 3 min (H–L) and topical exposure for 1 min (N–R) and 5 min (T–X). Panels A, G, M, and S are images of control, nonexposed rabbit eyes. Vapor exposure to the cornea caused thick bands and bright reflective areas, indicating severe corneal opacity. A similar pattern was observed after topical exposure, with growth of new vessels ( $\uparrow$ ) 21 and 28 days after acrolein treatment.  $n = 6$  rabbits in each group. All images were taken at  $7.1\times$  magnification. Scale bar = 3.0 mm.



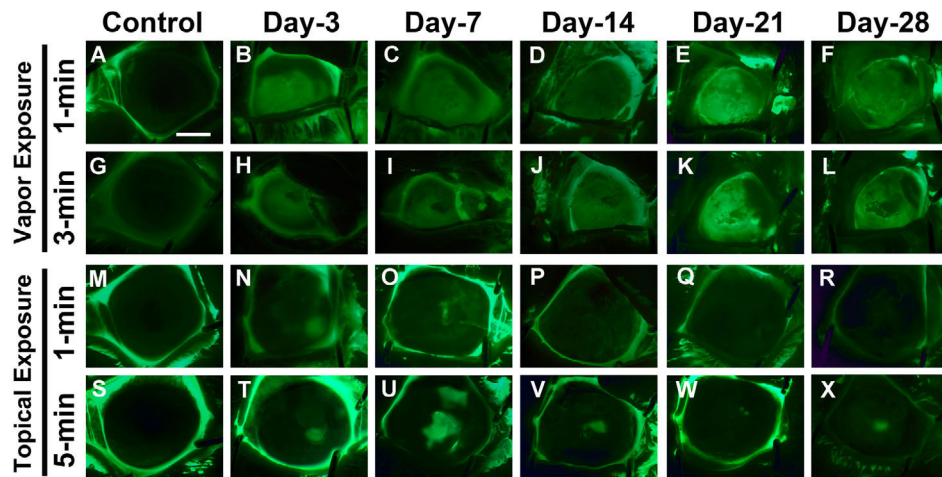


**Figure 4.**

*In vivo* fluorescein dye images showing a highly diffuse uptake of dye in the affected areas in the rabbit eyes after acrolein vapor exposure (1 min, B–F; and 3 min, H–L) and mildly diffused after acrolein topical exposure (1 min, N–R; and 5 min, T–X) at the tested times (30 min to 28 days). Vapor exposure to the cornea caused severe corneal abrasions and corneal surface defects, which fail to heal even at day 28 (F and L). A similar pattern was observed after topical exposure, with areas of severe corneal abrasions (N–P and T–V) that heal at a delayed rate up to day 28 (Q and R, and W and X).  $n = 6$  rabbits in each group. All images were taken at  $7.1\times$  magnification. Scale bar = 3.0 mm.

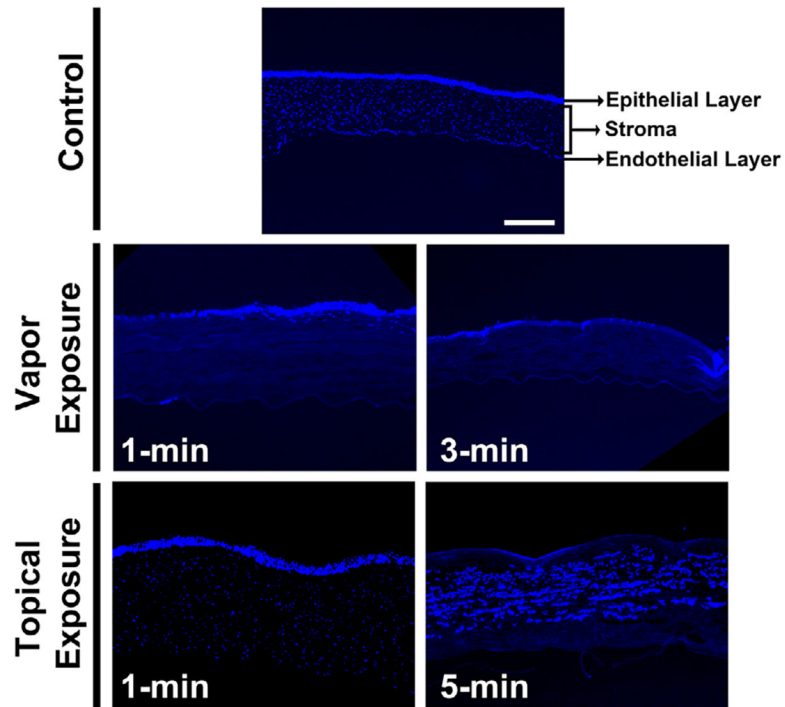


**Figure 5.** DAPI staining of the control and acrolein-exposed cornea sections showing nuclear staining/counts in the vapor-exposed (1 and 3 min) and topically exposed eyes (1 and 5 min) at day 28. Vapor exposure led to the loss of epithelial and stromal keratocytes in the 1-min exposure, which increased further in the 3-min exposed cornea. Similar observations were made in the corneas after topical treatment, except for the recovery of corneal epithelial cells in the 1-min exposed group and the mild recovery of epithelial cells and increased migration of inflammatory cells in the 5-min topical acrolein exposure group.  $n = 6$  rabbit eyes in each group. All images were taken at  $100\times$  magnification. Scale bar =  $100\ \mu\text{m}$ .

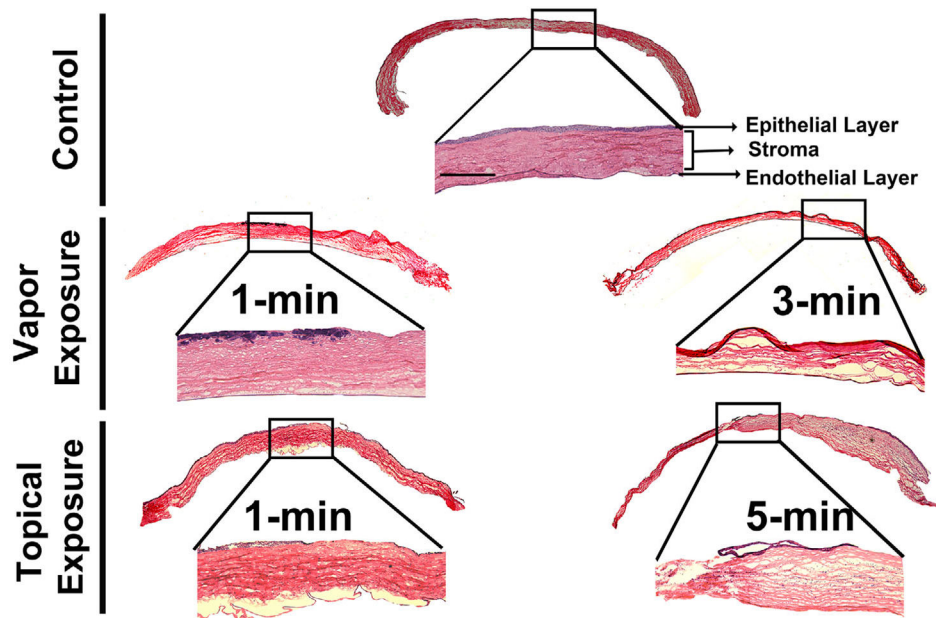


**Figure 6.** Hematoxylin and eosin staining of the corneal sections of the control and acrolein-exposed rabbit eyes at day 28. Vapor-treated corneas showed loss of epithelial cells in the anterior stroma in the 1-min exposed group. On the other hand, the 3-min exposed group caused severe disruption of the corneal stroma as well as epithelial cell loss. One-minute topical exposure caused corneal edema and loss of epithelial cells as well as distorted cellular architecture with increased pathology in the 5-min exposed group, accompanied by infiltrating inflammatory cells in the corneal stroma.  $n = 6$  rabbit eyes in each group. The entire corneal tissue section images are a montage of the 50 $\times$  magnification and inset images. Scale bar = 100  $\mu\text{m}$ . All inset images were taken at 100 $\times$  magnification.

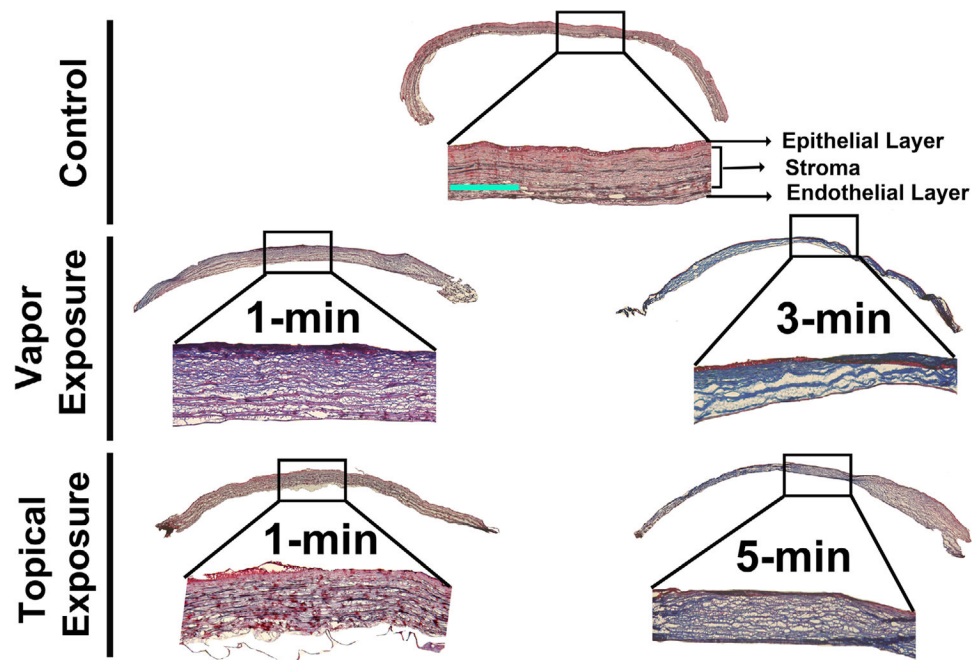


**Figure 7.** Masson's trichrome staining of the corneal sections of the control and acrolein-exposed rabbit eyes for the evaluation of corneal stromal collagen at day 28 after acrolein exposure. Vapor-treated corneas showed irregular collagen staining (collagen is stained blue) in the 1-min exposed group, which increased in staining intensity in the 3-min exposed group. The corneal collagens are highly disorganized and missing in certain areas due to the loss of corneal architecture. The topical exposure group showed similar collagen damage in the 1-min exposed cornea, with additional edema, and the staining intensity increased further in the 5-min exposed group, showing further damage and irregularity in the corneal collagens after acrolein exposure.  $n = 6$  rabbit eyes in each group. The entire corneal tissue section images are a montage of the 50 $\times$  magnification and inset images. Scale bar = 100  $\mu\text{m}$ . All inset images were taken at 100 $\times$  magnification.

**Table 1.** Clinical prognosis of corneal thickness, intraocular pressure (IOP), and tear flow after acrolein exposure

Group	Corneal thickness ( $\mu\text{m}$ )						IOP (mmHg)						Tear volume (mm)									
	Vapor exposure		Topical exposure		Vapor exposure		Topical exposure		Vapor exposure		Topical exposure		Vapor exposure		Topical exposure							
	1 min	3 min	1 min	5 min	1 min	3 min	1 min	5 min	1 min	3 min	1 min	5 min	1 min	3 min	1 min	5 min						
Control	354 $\pm$ 8.6	359 $\pm$ 6.7	348 $\pm$ 6.5	360 $\pm$ 5.6	10.0 $\pm$ 0.63	10.3 $\pm$ 0.88	10.5 $\pm$ 0.76	10.7 $\pm$ 0.33	13.5 $\pm$ 0.76	14.2 $\pm$ 0.54	13.3 $\pm$ 0.80	13.2 $\pm$ 0.95	504 $\pm$ 6.2	504 $\pm$ 6.4	495 $\pm$ 7.9	495 $\pm$ 7.7	12.7 $\pm$ 0.39	12.7 $\pm$ 0.39	27.6 $\pm$ 0.91	32.0 $\pm$ 0.88	17.3 $\pm$ 0.51	17.3 $\pm$ 0.70
30 min	490 $\pm$ 13.5	501 $\pm$ 15.4	648 $\pm$ 18.9	628 $\pm$ 16.9	22.0 $\pm$ 1.46	23.7 $\pm$ 0.76	12.8 $\pm$ 0.65	11.3 $\pm$ 1.20	26.3 $\pm$ 1.88	27.7 $\pm$ 0.76	20.5 $\pm$ 1.73	20.5 $\pm$ 1.84	490 $\pm$ 13.5	501 $\pm$ 15.4	648 $\pm$ 18.9	628 $\pm$ 16.9	12.8 $\pm$ 0.65	11.3 $\pm$ 1.20	26.3 $\pm$ 1.88	27.7 $\pm$ 0.76	20.5 $\pm$ 1.73	20.5 $\pm$ 1.84
Day 1	497 $\pm$ 7.7	536 $\pm$ 11.1	767 $\pm$ 19.2	843 $\pm$ 5.2	22.2 $\pm$ 0.48	22.3 $\pm$ 0.92	11.0 $\pm$ 0.37	11.0 $\pm$ 0.82	20.1 $\pm$ 0.60	23.0 $\pm$ 0.97	13.5 $\pm$ 1.69	10.7 $\pm$ 1.26	497 $\pm$ 3.4	543 $\pm$ 12.1	756 $\pm$ 18.3	858 $\pm$ 11.9	10.3 $\pm$ 0.42	9.8 $\pm$ 0.54	12.5 $\pm$ 1.84	14.0 $\pm$ 1.03	12.7 $\pm$ 1.91	8.8 $\pm$ 1.11
Day 3	519 $\pm$ 5.4	559 $\pm$ 8.9	745 $\pm$ 14.5	738 $\pm$ 14.9	11.7 $\pm$ 0.92	15.2 $\pm$ 1.40	10.3 $\pm$ 0.67	10.5 $\pm$ 0.76	8.3 $\pm$ 0.80	9.0 $\pm$ 1.59	9.1 $\pm$ 0.61	6.7 $\pm$ 0.84	519 $\pm$ 5.4	559 $\pm$ 8.9	745 $\pm$ 14.5	738 $\pm$ 14.9	10.3 $\pm$ 0.67	10.5 $\pm$ 0.76	8.3 $\pm$ 0.80	9.0 $\pm$ 1.59	9.1 $\pm$ 0.61	6.7 $\pm$ 0.84
Day 7	530 $\pm$ 11.1	614 $\pm$ 15.5	721 $\pm$ 17.4	722 $\pm$ 15.9	10.2 $\pm$ 0.40	11.7 $\pm$ 0.56	10.8 $\pm$ 0.70	10.0 $\pm$ 0.58	11.0 $\pm$ 1.15	9.5 $\pm$ 1.09	6.5 $\pm$ 0.76	7.8 $\pm$ 0.95	530 $\pm$ 11.1	614 $\pm$ 15.5	721 $\pm$ 17.4	722 $\pm$ 15.9	10.8 $\pm$ 0.70	10.0 $\pm$ 0.58	11.0 $\pm$ 1.15	9.5 $\pm$ 1.09	6.5 $\pm$ 0.76	7.8 $\pm$ 0.95
Day 21	513 $\pm$ 7.3	628 $\pm$ 16.8	692 $\pm$ 15.9	716 $\pm$ 15.6	11.2 $\pm$ 0.40	12.5 $\pm$ 0.50	10.5 $\pm$ 0.56	10.2 $\pm$ 0.48	10.5 $\pm$ 1.09	8.7 $\pm$ 1.31	7.2 $\pm$ 0.70	6.5 $\pm$ 1.06	513 $\pm$ 7.3	628 $\pm$ 16.8	692 $\pm$ 15.9	716 $\pm$ 15.6	10.5 $\pm$ 1.09	10.2 $\pm$ 0.48	10.5 $\pm$ 1.09	8.7 $\pm$ 1.31	7.2 $\pm$ 0.70	6.5 $\pm$ 1.06

<sup>a</sup>  $P < 0.05$ ;  $**P < 0.01$ ;  $***P < 0.001$ .

*ns*, not significant.